Original Article

The value of blood flow velocity and pressure gradient in differentiating patients with different types of heart failure

Jiaxuan Guo[1,2], Xiuzheng Yue[3], Wenying Liang[1,2], Lirong Ma[1,2], Xiao Sun[1], Huairong Zhang[1], Li Zhu[1]

[1]Department of Radiology, General Hospital of Ningxia Medical University, Yinchuan, China; [2]The First Clinical Medical College of Ningxia Medical University, Yinchuan, China; [3]Philips Healthcare, Beijing, China

Contributions: (I) Conception and design: J Guo, L Zhu; (II) Administrative support: X Yue, L Zhu; (III) Provision of study materials or patients: W Liang, H Zhang, L Zhu; (IV) Collection and assembly of data: J Guo, L Ma; (V) Data analysis and interpretation: J Guo, X Yue, X Sun, L Zhu; (VI) Manuscript writing: All authors; (VII) Final approval of manuscript: All authors.

Correspondence to: Li Zhu, MD, PhD. Department of Radiology, General Hospital of Ningxia Medical University, 804 South Shengli Street, Yinchuan 750004, China. Email: zhuli72@163.com.

Background: Patients with different types of heart failure (HF) exhibit varying rates of blood flow through cardiac chambers and pressure gradients across the aortic valve, attributed to differing degrees of myocardial contractility. Assessment of these dynamics offers insights into early HF diagnosis. This study aimed to analyze left ventricular outflow tract (LVOT) blood flow parameters, specifically peak blood flow velocity and pressure gradient derived from four-dimensional flow cardiovascular magnetic resonance (4D flow CMR), and to evaluate 4D flow CMR's utility in distinguishing HF types.

Methods: This prospective cross-sectional study recruited 115 HF patients from January 2019 to May 2022 at the General Hospital of Ningxia Medical University, classified by the New York Heart Association Cardiac Function Classification of Heart Failure as class II–IV, alongside a control group (n=30). Participants underwent cardiovascular magnetic resonance (CMR), including 4D flow. HF patients were categorized into heart failure with reduced ejection fraction (HFrEF, n=55), heart failure with mildly reduced ejection fraction (HFmrEF, n=30), and heart failure with preserved ejection fraction (HFpEF, n=30), based on ejection fraction. The cardiac functional parameters and aortic valve flow indices were measured using Circle Cardiovascular Imaging. LVOT 4D flow data were obtained 3 mm below the junction of the aortic valve leaflets, assessing peak velocities above and below the valve. Differences in cardiac function and blood flow parameters between groups were analyzed using one-way analysis of variance (ANOVA). The accuracy of these parameters in identifying subgroups was assessed using the receiver operating characteristic (ROC) curve.

Results: Analysis of conventional cardiac function parameters revealed that left ventricular ejection fraction (LVEF) was significantly lower in the HFrEF and HFmrEF groups compared to the HFpEF and control groups (P<0.01). Additionally, end-diastolic volume and end-systolic volume were significantly higher in the HFrEF and HFmrEF groups than in the HFpEF and control groups (P<0.01). However, there were no significant differences in cardiac function parameters between the HFpEF and control groups (P>0.05). Significant differences were observed in aortic valve peak pressure gradients (Supra-APGmax) among the four study groups (5.01±1.09 *vs.* 6.23±2.94 *vs.* 7.63±1.81 *vs.* 8.89±2.97 mmHg, P<0.05). Aortic valve peak velocities in the HFrEF group differed significantly from the HFpEF and control groups (111.31±12.05 cm/s *vs.* 137.2±16 *vs.* 147.15±24.55 cm/s, P<0.001). The ROC curve for the pressure gradient below the aortic valve had an area under the curve (AUC) of 0.728 [95% confidence interval (CI): 0.591–0.864, P=0.002], with an optimal threshold of 4.72 mmHg (sensitivity: 0.8, specificity: 0.7, Youden index: 0.5).

Conclusions: HF patients exhibit reduced pressure gradients across the aortic valve during systole, indicative of altered intracardiac blood flow dynamics. Combining aortic valve velocities and pressure gradients can aid in distinguishing different types of HF, including HFpEF patients.

Keywords: Heart failure (HF); four-dimensional flow (4D flow); left ventricular outflow tract (LVOT); cardiovascular magnetic resonance (CMR)

Submitted Feb 18, 2024. Accepted for publication Aug 15, 2024. Published online Sep 26, 2024.
doi: 10.21037/qims-24-311
View this article at: https://dx.doi.org/10.21037/qims-24-311

Introduction

Heart failure (HF) results from structural or functional abnormalities in the heart, affecting the relaxation or contraction processes of the ventricles and giving rise to complex clinical syndromes (1). Impairments and remodeling of the left ventricle (LV) may occur gradually before clinical symptoms become apparent, highlighting the critical need for precise and early diagnostic methods. Currently, transthoracic Doppler ultrasound remains the preferred tool for assessing left ventricular ejection fraction (LVEF), contractile function, and blood flow patterns (2). However, limitations such as operator-dependent variability and acoustic window constraints reduce the accuracy of ultrasound measurements of cardiac blood flow parameters. Moreover, the diagnosis and classification of HF patients heavily rely on ultrasound-based LVEF measurements (3). For patients with heart failure with preserved ejection fraction (HFpEF), diagnosis requires integrating clinical symptoms, signs, and brain natriuretic peptide testing, which may lead to underdiagnosis by less experienced clinicians (4). In contrast, four-dimensional flow cardiovascular magnetic resonance (4D flow CMR) represents a novel technique that enables three-dimensional (3D) velocity encoding (VENC) and visualization of blood flow patterns within the heart and major blood vessels (5-7). With its high temporal resolution, 4D flow CMR allows detailed study of blood flow patterns in specific regions of the LV throughout the cardiac cycle, such as the left ventricular outflow tract (LVOT) (8-10).

Certain researchers have demonstrated that left ventricular blood flow patterns closely correlate with myocardial, valve, and large blood vessel morphology and movement, potentially serving as sensitive indicators of cardiac functional impairments, including HF (11). For example, van Ooij *et al.* utilized 4D flow CMR to quantify pressure gradients in the LVOT, revealing that peak systolic pressure differences in hypertrophic cardiomyopathy patients (21±16 mmHg) significantly exceeded those in the control group (9±2 mmHg) (12). This underscores the relevant association between abnormal LVOT blood flow, increased left ventricular load, and adverse myocardial remodeling. However, quantitative analysis of blood flow patterns in various HF subtypes using LVOT 4D flow CMR and their relationship with systolic left ventricular dysfunction remains limited.

Therefore, this study aimed to compare aortic valve blood flow velocities and pressure gradients among different subtypes of HF patients and analyze the correlation between these parameters and systolic left ventricular dysfunction. We present this article in accordance with the STROBE reporting checklist (available at https://qims.amegroups.com/article/view/10.21037/qims-24-311/rc).

Methods

Study population

The primary aim of this study was to assess the feasibility of using 4D flow CMR to distinguish between different types of HF. Patients diagnosed with HF between January 2019 and May 2022 at Ningxia Medical University General Hospital were prospectively enrolled for cardiovascular magnetic resonance (CMR) examination. These HF patients met the diagnostic criteria established by the European Society of Cardiology in 2021 (3) and underwent comprehensive CMR, echocardiography, and electrocardiography. Both cine and 4D flow CMR images obtained were of satisfactory quality. Heart failure with reduced ejection fraction (HFrEF) was defined as LVEF ≤40%, indicating significant decline in left ventricular systolic function; heart failure with mildly reduced ejection fraction (HFmrEF) was defined as 41%≤ LVEF ≤49%, indicating mild reduction in left ventricular systolic function; HFpEF was defined as patients with HF symptoms and signs, cardiac structural and/or functional abnormalities, and/or elevated levels of brain natriuretic peptide, with LVEF ≥50% (13). *Table 1* presents the general characteristics of the study population. Exclusion criteria for HF patients included conditions such as hypertrophic cardiomyopathy, aortic valve insufficiency or stenosis, hypertension, diabetes, malignant cardiac tumors, claustrophobia, presence of implanted or metal medical

Table 1 Comparison of general characteristics among study groups

Clinical information	HFrEF (n=55)	HFmrEF (n=30)	HFpEF (n=30)	Control (n=30)	F/H/c^2	P value
Age (years)	45.93±14.3*	47.6±15.63*	42.8±16.12	36.6±15.22	3.29	0.023
Sex (male)	42 (76.4%)	25 (83.3%)	17 (56.7%)	22 (73.3%)	6.017	0.111
BMI (kg/m^2)	24.73±3.54†	23.94±2.56	24.63±2.95	23.1±1.94	3.272	0.026
BSA (m^2)	1.93±0.2	1.93±0.15	1.87±0.16	1.9±0.18	1.114	0.346
HR (bpm)	78.2±14.11‡	72.53±11.41	65.97±9.06*	72.73±15.15	7.846	<0.001
NYHA class					8.197	0.414
II	22 (40%)	13 (43.3%)	15 (50%)	–		
III	17 (30.9%)	9 (30%)	10 (33.3%)	–		
IV	7 (12.7%)	1 (3.3%)	2 (6.7%)	–		
NT-proBNP (pg/mL)	667.02±574.23	504.45±185.25	450.83±174.21	–	2.956	0.057

Data are reported as mean ± standard deviation or number (%). *, significantly different from the control group, P<0.05; †, significantly different between HFrEF and HFmrEF groups, P<0.05; ‡, significantly different from HFpEF group, P<0.05. HFrEF, heart failure with reduced ejection fraction; HFmrEF, heart failure with mildly reduced ejection fraction; HFpEF, heart failure with preserved ejection fraction; BMI, body mass index; BSA, body surface area; HR, heart rate; bpm, beats per minute; NYHA, New York Heart Association functional class (II: slight limitation of physical activity; III: marked limitation of physical activity due to heart disease; IV: inability to carry on any physical activity); NT-proBNP, N-terminal pro-brain natriuretic peptide.

devices, and significant arrhythmias at enrollment. The process of case-specific natriuresis is shown in *Figure 1*. A control group of healthy volunteers without history of cardiovascular diseases, liver or kidney dysfunction, immune disorders, neurological disorders, metabolic diseases, malignant tumors, long-term medication use, smoking, or alcohol consumption was also recruited. These volunteers underwent echocardiography and CMR examinations. The study was conducted in accordance with the Declaration of Helsinki (as revised in 2013). The study was approved by the Research Ethics Committee of Ningxia Medical University General Hospital (approval No. KYLL-2021-255) and the requirement for individual consent for this analysis was waived due to retrospective nature of this study.

Equipment and methods

(I) Cardiac ultrasound examination: this study utilized a Philips IE33 color Doppler ultrasound system (Philips Healthcare, Best, Netherlands) equipped with an S5-1 phased array probe (frequency 1–5 MHz). Offline image acquisition and analysis were conducted using the Tom Tec 4.0 workstation (TomTec Imaging Systems, Unterschleissheim, Germany). The frame rate of the instrument was adjusted to >60 frames/second after positioning, and electrocardiogram (ECG) data were acquired over three cardiac cycles. Following measurements, LVEF was calculated using the biplane Simpson's method. Systolic LVOT flow velocity was assessed at the aortic valve to estimate the maximum pressure gradient across the LVOT (LVOT-PG).

(II) Magnetic resonance imaging (MRI): patients underwent cardiac scanning using a 3.0T MRI system (Philips Healthcare, Netherlands). Uniform sequence parameters were applied across all cases. Steady-state free precession cine sequences were employed for measuring cardiac functional parameters in a short-axis orientation, with scan parameters including echo time (TE) of 1.28 ms, repetition time (TR) of 2.6 ms, flip angle of 45°, field of view (FOV) of 350×350×100 mm, and slice thickness of 8 mm. Voxel dimensions were 2×2×8 mm, with 30 phases collected per cardiac cycle. Three-chamber 4D flow CMR acquisitions were performed during free-breathing, covering the entire cardiac cycle without respiratory gating. The time resolution was typically 35–45 ms, capturing 20–25 phases depending on heart rate, and reconstructed into 40 cardiac phases. Typical scan parameters included TE/TR of 1.2/2.0 ms, flip angle of 8°, acquisition and reconstruction voxel size of 2.5×2.5×2.5 mm, with a selected flow VENC of 200 cm/s based on literature recommendations (14).

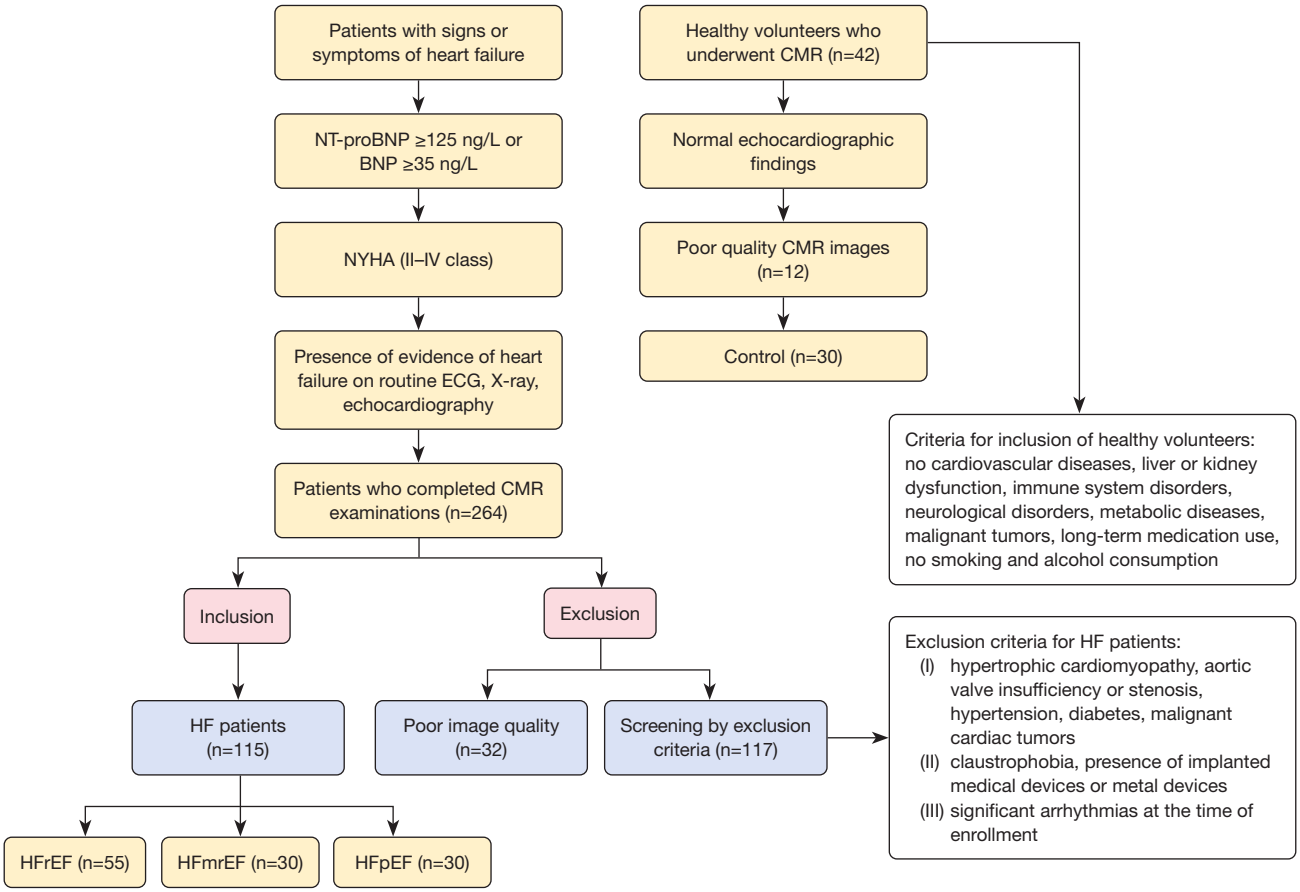

Figure 1 Workflow chart for inclusion and exclusion of heart failure patients and healthy controls. NT-proBNP, N-terminal pro-brain natriuretic peptide; BNP, brain natriuretic peptide; NYHA, New York Heart Association Cardiac Function Classification; ECG, electrocardiogram; CMR, cardiovascular magnetic resonance; HF, heart failure; HFrEF, heart failure with reduced ejection fraction; HFmrEF, heart failure with mildly reduced ejection fraction; HFpEF, heart failure with preserved ejection fraction.

Image post-processing

Post-processing and analysis of images were conducted using the cvi42 post-processing software (Version 5.13.10; Circle Cardiovascular Imaging, Calgary, Canada). Measurement of cardiac function: In the short-axis cine sequences, the software automatically delineated the endocardial and epicardial boundaries of the LV based on the American Heart Association (AHA) myocardial segmentation model (1), excluding papillary muscle contours. Manual adjustments were made to correct any irregular contours. The software computed left ventricular end-diastolic volume (LVEDV), left ventricular end-systolic volume (LVESV), LVEF, stroke volume (SV), and other cardiac functional parameters. Measurement of blood flow parameters: after importing the 4D flow CMR data, regions of interest were selected within the module. Masks were manually adjusted to exclude fat and gas tissues, followed by displacement correction and anti-aliasing. Utilizing 3D rendering, standard images of the left ventricular inflow and outflow planes were generated and saved. A sample plane was positioned at the level of the aortic valve, perpendicular to the blood flow direction. The software plotted the average velocity-time curve of blood flow throughout the cardiac cycle. Refer to *Figure 2* for detailed positioning guidelines. The plane was positioned 3 mm above and below the junction of the three leaflets of the aortic valve, measuring peak velocities above and below the aortic valve. 4D flow CMR captured VENC data in three directions, producing 3D phase images with high temporal resolution. Peak systolic velocity above the aortic valve (Supra-AVmax), peak systolic velocity below the aortic valve (Sub-

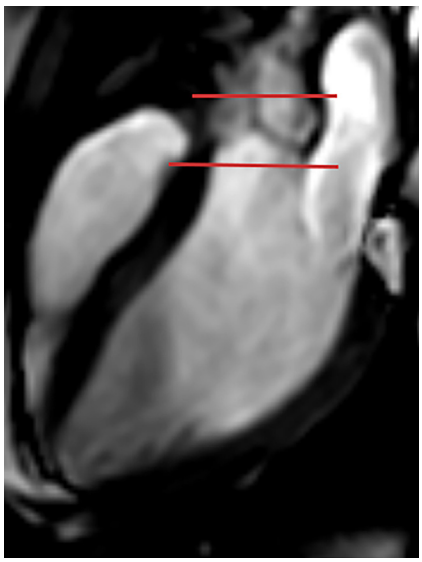

Figure 2 Illustration of aortic valve plane placement. Two red lines denote the position of the plane, which is positioned 3 mm above and below the junction of the three leaflets of the aortic valve. This setup allows for accurate measurement of blood flow dynamics in relation to the aortic valve.

AVmax), and the estimated maximum instantaneous pressure gradient through the aortic valve (APGmax) were recorded using a simplified Bernoulli equation ($\Delta P=4V^2max$) (15). The aortic valve velocity in the LVOT directly reflects ventricular pumping function, whereas the aortic valve pressure gradient indicates cardiac ejection efficiency (16). The measurement process was performed by two clinical doctors each with at least two years of software experience, and the average of their results was recorded.

Statistical analysis

Data analysis was conducted using the statistical software SPSS 26.0 (IBM Corp., Armonk, NY, USA), with GraphPad Prism 9.0 (GraphPad Software, San Diego, CA, USA) utilized for graphical representation. The Shapiro-Wilk test assessed data normality. Normally distributed or approximately normally distributed quantitative data were presented as mean ± standard deviation. Skewed distributed quantitative data were expressed as median (interquartile range). Categorical data were reported as counts (percentages). One-way analysis of variance (ANOVA) compared normally distributed quantitative data; in cases of heterogeneous variances, Welch's test (adjusted F-test) was applied, followed by post hoc least significant difference (LSD) tests for pairwise comparisons. Mann-Whitney U test compared severely skewed quantitative data, with nonparametric pairwise comparisons for post hoc analysis. Chi-square test assessed categorical variables. Bivariate linear and rank correlation analyses were conducted for parameters with significant differences. Binary logistic regression explored factors influencing HFpEF occurrence. Receiver operating characteristic (ROC) analysis evaluated the accuracy of blood flow parameters in subgroup identification. Cases with missing data were excluded. A P value <0.05 (two-sided) indicated statistical significance. Additionally, CMR examinations were performed on healthy controls using the same MRI machine at the hospital over a two-year period, synchronized with the collection time of the case group.

Results

Basic characteristics of the study population

A total of 115 HF patients participated in the study (HFrEF, n=55; HFmrEF, n=30; HFpEF, n=30), ranging in age from 18 to 79 years, including 84 males. The control group consisted of 30 individuals aged 14–75 years, including 22 males. Both the HFrEF and HFmrEF groups were older compared to the healthy control group. There were no significant differences in body mass index (BMI), body surface area (BSA), and NT-proBNP levels among the HF groups when compared to the control group. New York Heart Association (NYHA) functional class distribution did not significantly differ among the groups, with the majority of HFrEF, HFmrEF, and HFpEF patients classified as NYHA class II (40%, 43.3%, and 50%, respectively). *Table 1* presents the general characteristics of the study population.

Comparison of echocardiography and CMR parameters

In the echocardiography analysis, LVEF in the HFrEF and HFmrEF groups was significantly lower compared to the HFpEF and control groups [HFrEF *vs.* HFmrEF *vs.* HFpEF *vs.* control =31.3% (24%, 35.2%) *vs.* 44.4% (41.6%, 47%) *vs.* 55% (52.9%, 57.2%) *vs.* 60.2% (51.7%, 65.9%), P<0.01]. Additionally, no significant differences were found in LVEDV between the HFrEF and HFmrEF groups [219.8 (166.6, 263.7) *vs.* 166.6 (141.3, 210.4) mL, P=0.807], or between the HFpEF and control groups [112.8 (90.1, 129.5) *vs.* 102.4 (92.5, 118.2) mL, P>0.99]. Similarly, no significant differences

Table 2 Comparison of echocardiography and CMR parameters among study groups

Cardiac function parameters	HFrEF	HFmrEF	HFpEF	Control	H/F	P value
Echocardiography						
LVEF (%)	31.3 (24, 35.2)*†‡	44.4 (41.6, 47)*‡	55 (52.9, 57.2)	60.2 (51.7, 65.9)	116.199	<0.001
LVEDV (mL)	219.8 (166.6, 263.7)*‡	166.6 (141.3, 210.4)*‡	112.8 (90.1, 129.5)	102.4 (92.5, 118.2)	64.519	<0.001
LVESV (mL)	135.4 (89.5, 180)*‡	78.6 (58.1, 115.6)*‡	37.9 (24.6, 45.8)	35 (29.6, 41)	76.885	<0.001
SV (mL)	78.11±18.63	87.06±18.09*†	72.83±20.43	73.29±19.11	2.669	0.051
Cardiac magnetic resonance						
LVEF (%)	24.2 (19.7, 27.3)*†‡	43.2 (38.5, 45.2)*‡	60.6 (55.5, 63.4)	59.4 (58.2, 66.8)	93.33	<0.001
LVEDV (mL)	250 (218.4, 309.4)*†‡	160.3 (140.8, 226.1)*	145.1 (130.3, 157.4)	112.5 (101, 132.6)	115.702	<0.001
LVESV (mL)	189.2 (161.4, 244.6)*†‡	96.5 (73.8, 135.4)*‡	63 (47.6, 70.1)	45.8 (33.5, 55.5)	124.715	<0.001
SV (mL)	61.02±16.43*‡	76.33±19.62	82.76±9.98	76.04±15.04	14.889	<0.001

Data are reported as mean ± standard deviation, if normally distributed, or as median (interquartile range) otherwise. *, significantly different from the control group, P<0.05; †, significantly different between HFrEF and HFmrEF groups, P<0.05; ‡, significantly different from HFpEF group, P<0.05. CMR, cardiovascular magnetic resonance; HFrEF, heart failure with reduced ejection fraction; HFmrEF, heart failure with mildly reduced ejection fraction; HFpEF, heart failure with preserved ejection fraction; H/F, H stands for the test statistic of Kruskal-Wallis Test, F stands for the statistic of analysis of variance (ANOVA); LVEF, left ventricular ejection fraction; LVEDV, left ventricular end-diastolic volume; LVESV, left ventricular end-systolic volume; SV, stroke volume.

were noted in LVESV between the HFrEF and HFmrEF groups [135.4 (89.5, 180) *vs.* 78.6 (58.1, 115.6) mL, P=0.226], or between the HFpEF and control groups [37.9 (24.6, 45.8) *vs.* 35 (29.6, 41) mL, P>0.99], but significant differences were observed in pairwise comparisons among the other groups (P<0.05).

In the CMR examination, there were no significant differences in LVEF between the HFpEF group and the control group [60.6 (55.5, 63.4)% *vs.* 59.4 (58.2, 66.8)%, P>0.99], but significant differences were observed in pairwise comparisons among the remaining groups (P<0.001). Similarly, no significant differences were observed in LVEDV between the HFpEF group and the control group [145.1 (130.3, 157.4) *vs.* 112.5 (101, 132.6) mL, P=0.528], but significant differences were seen in pairwise comparisons among the other groups (P<0.05). Furthermore, no significant differences were found in LVESV between the HFpEF group and the control group [63 (47.6, 70.1) *vs.* 45.8 (33.5, 55.5) mL, P=0.508], but significant differences were observed in pairwise comparisons among the other groups (P<0.05). Detailed comparisons of echocardiography and CMR parameters are presented in *Table 2*.

LVOT 4D flow CMR measurements of velocity and pressure gradient analysis

The intracardiac blood flow patterns for each group are illustrated in *Figure 3*. Further analysis of ultrasound-derived aortic valve peak velocity and pressure gradient revealed no significant differences between the HF groups and the control group (P=0.222, P=0.165), as detailed in *Table 3*. However, in the CMR examination, peak aortic valve pressure gradients showed an increasing trend: HFrEF versus HFmrEF (5.01±1.09 *vs.* 6.23±2.94 mmHg, P=0.031), HFpEF versus control (7.63±1.81 *vs.* 8.89±2.97 mmHg, P=0.019), and HFmrEF versus HFpEF (6.23±2.94 *vs.* 7.63±1.81 mmHg, P=0.007). Significant differences were also observed in pairwise comparisons among other groups (P<0.001). There were no significant differences in aortic valve peak velocity between the HFrEF and HFmrEF groups (111.31±12.05 *vs.* 119.91±35.17 cm/s, P=0.154), nor between the HFpEF and control groups (137.2±16 *vs.* 147.15±24.55 cm/s, P=0.069). However, peak aortic valve velocity was significantly lower in the HFmrEF group compared to the HFpEF group (119.91±35.17 *vs.* 137.2±16 cm/s, P=0.001), as well as in pairwise comparisons with other groups (P<0.001). Regarding aortic valve peak velocity, the HFrEF group was significantly lower than the control group (104.73±14.8 *vs.* 130.99±28.52 cm/s, P<0.001), the HFmrEF group was significantly lower than the control group (107.31±19.42 *vs.* 130.99±28.52 cm/s, P<0.001), and the HFpEF group was also significantly lower than the control group (112.47±17.34 *vs.* 130.99±28.52 cm/s, P<0.001). Similarly, for Sub-

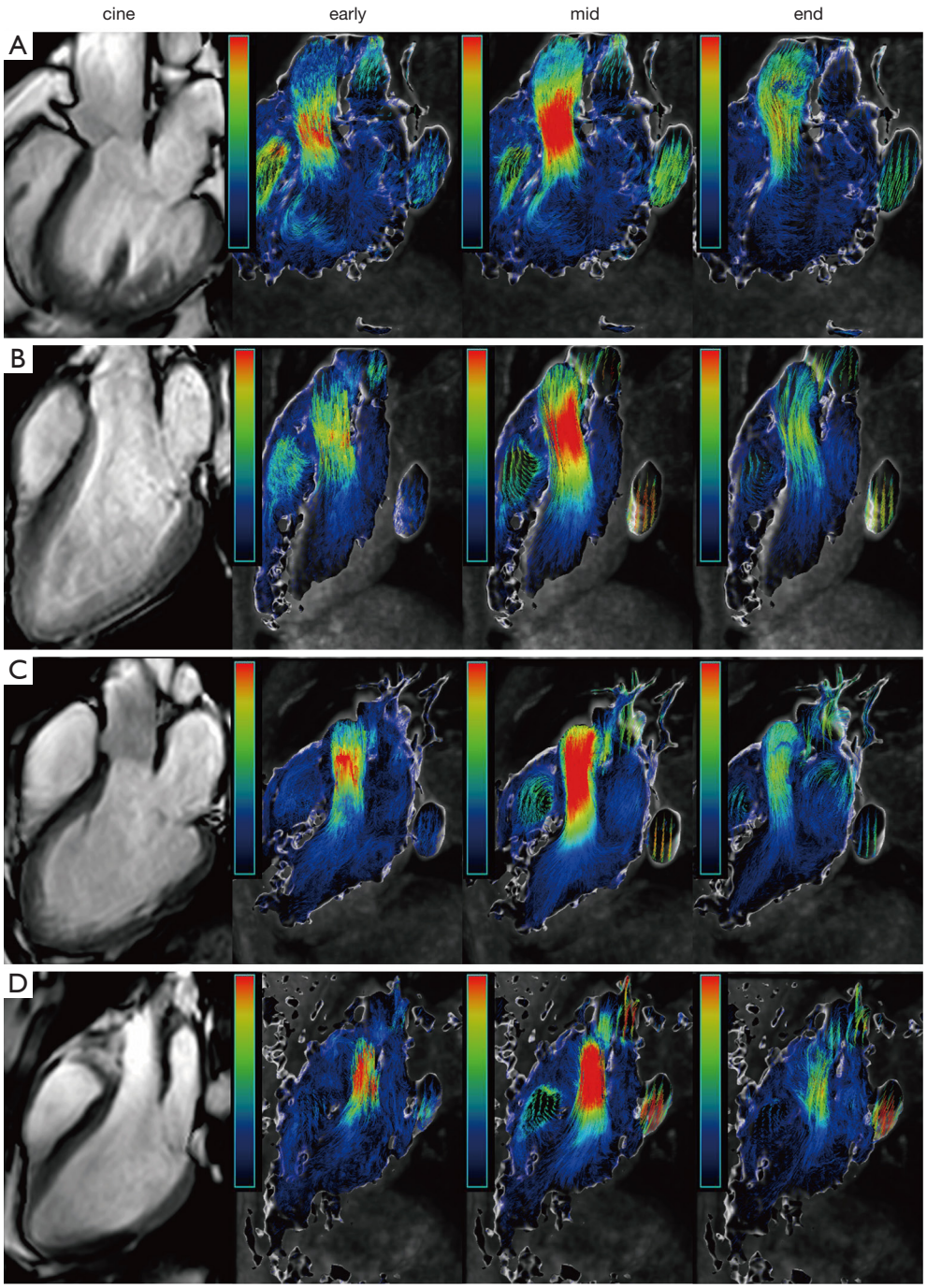

Figure 3 Plot of blood flow patterns in different study populations. (A) 4D flow CMR blood flow patterns in a patient with HFrEF during early, mid, and end systole. (B) 4D flow CMR blood flow patterns in a patient with HFmrEF during early, mid, and end systole. (C) 4D flow CMR blood flow patterns in a patient with HFpEF during early, mid, and end systole. (D) 4D flow CMR blood flow patterns in a health volunteer during early, mid, and end systole. 4D, four-dimensional; CMR, cardiovascular magnetic resonance; HFrEF, heart failure with reduced ejection fraction; HFmrEF, heart failure with mildly reduced ejection fraction; HFpEF, heart failure with preserved ejection fraction.

Table 3 Comparison of intracavitary hemodynamic parameters in different types of HF patients

Blood flow parameters	HFrEF	HFmrEF	HFpEF	Control	F	P value
Ultrasound						
Supra-AVmax (cm/s)	104.6±19.3	106.36±20.83	95.79±25.24	108.53±15.17	1.489	0.222
Supra-APGmax (mmHg)	4.67±1.83	5.14±2.02	5.67±2.27	4.92±1.34	1.725	0.165
CMR						
Supra-AVmax (cm/s)	111.31±12.05*‡	119.91±35.17*‡	137.2±16	147.15±24.55	32.557	<0.001
Sub-AVmax (cm/s)	104.73±14.8*	107.31±19.42*	112.47±17.34*	130.99±28.52	7.782	<0.001
Supra-APGmax (mmHg)	5.01±1.09	6.23±2.94	7.63±1.81	8.89±2.97	29.8	<0.001
Sub-APGmax (mmHg)	4.47±1.27*	4.75±1.81*	5.18±1.74*	7.18±3	7.811	<0.001

Data are reported as mean ± standard deviation. *, significantly different from the control group, P<0.05; ‡, significantly different from HFpEF group, P<0.05. HF, heart failure; HFrEF, heart failure with reduced ejection fraction; HFmrEF, heart failure with mildly reduced ejection fraction; HFpEF, heart failure with preserved ejection fraction; F, the statistic of analysis of variance (ANOVA); Supra-AVmax, aortic valve peak velocity; Sub-AVmax, aortic valve subvalvular velocity; Supra-APGmax, aortic valve peak pressure gradient; Sub-APGmax, aortic valve subvalvular pressure gradient; CMR, cardiovascular magnetic resonance.

APGmax, the HFrEF group was significantly lower than the control group (4.47±1.27 *vs.* 7.18±3 mmHg, P<0.001), the HFmrEF group was significantly lower than the control group (4.75±1.81 *vs.* 7.18±3 mmHg, P<0.001), and the HFpEF group was significantly lower than the control group (5.18±1.74 *vs.* 7.18±3 mmHg, P<0.001). Detailed results are presented in *Table 3* and *Figure 4*.

Analysis of blood flow parameters and cardiac function parameters relationship

In further correlation analysis, a positive relationship was found between Supra-APGmax and LVEF (r=0.593, P<0.001). Additionally, as illustrated in *Figure 5*, Supra-APGmax was negatively correlated with both LVEDV and LVESV (r=–0.539, r=–0.603, P<0.001).

ROC curve analysis of blood flow parameters

Figure 6 illustrates the value of the aortic valve gradient in distinguishing between the HFpEF group and the control group. The area under the curve (AUC) for the pressure gradient across the aortic valve was 0.659 [95% confidence interval (CI): 0.517–0.801, P=0.035], with an optimal threshold of 10.63 mmHg (sensitivity: 0.367, specificity: 1, Youden index: 0.367). Similarly, for the pressure gradient below the aortic valve, the AUC was 0.728 (95% CI: 0.591–0.864, P=0.002), with an optimal threshold of 4.72 mmHg (sensitivity: 0.8, specificity: 0.7, Youden index: 0.5).

Discussion

In this study, 4D flow technology was utilized to visualize blood flow in HF patients, focusing on quantitative analysis of blood flow in the LVOT. The findings suggest that distinguishing between different HF patient types cannot be solely achieved through the use of LVEF and end-diastolic volume, especially in distinguishing HFpEF patients from the healthy control group. However, effective differentiation among HF patient types was demonstrated through the utilization of systolic aortic valve velocity and transvalvular pressure gradient derived from 4D flow. This not only aids in clinical treatment decisions but also holds prognostic value for long-term follow-up.

Currently, HF is classified into three types based on LVEF (13), each associated with distinct prognostic characteristics. Despite significant advances in pharmacological and device-based therapies for HFrEF, the prognosis for many patients remains poor, with high mortality risks (17). Studies also indicate that although symptomatic control can be achieved in HFpEF patients, there is no treatment proven to improve survival rates, and mortality rates have remained unchanged over the past two decades (18). Additionally, research on all-cause mortality rates among HFrEF, HFmrEF, and HFpEF events suggests that HFmrEF and HFrEF patients have poorer survival rates compared to HFpEF patients (19). Therefore, accurate differentiation of HF patients at high clinical risk is crucial. However, distinguishing between different HF types requires a systematic evaluation. A novel method

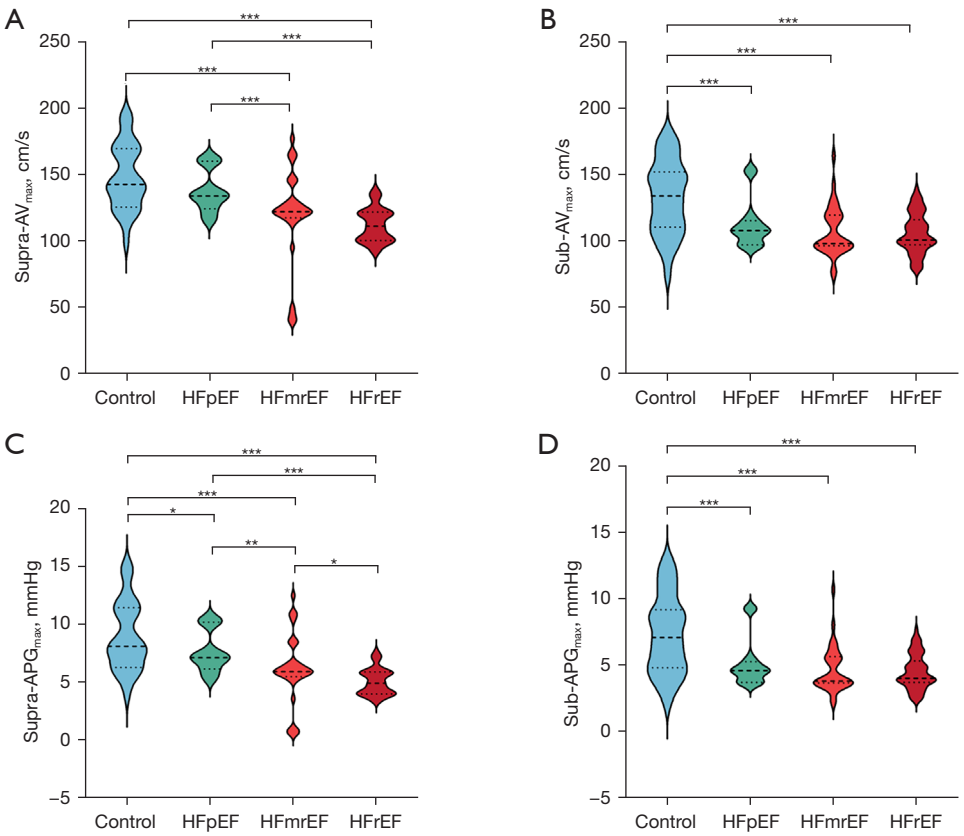

Figure 4 Comparison of cardiac magnetic resonance aortic valve peak velocity and pressure gradient differences between groups. (A) One-way ANOVA was used to analyze the variability of Supra-AVmax between groups of people. (B) One-way ANOVA was used to analyze the variability of Sub-AVmax between groups of people. (C) One-way ANOVA was used to analyze the variability of Supra-APGmax between groups of people. (D) One-way ANOVA was used to analyze the variability of Sub-APGmax between groups of people. *, P<0.05; **, P<0.01; ***, P<0.001. HFpEF, heart failure with preserved ejection fraction; HFmrEF, heart failure with mildly reduced ejection fraction; HFrEF, heart failure with reduced ejection fraction; Supra-AVmax, aortic valve peak velocity; Sub-AVmax, aortic valve subvalvular velocity; Supra-APGmax, aortic valve peak pressure gradient; Sub-APGmax, aortic valve subvalvular pressure gradient; ANOVA, analysis of variance.

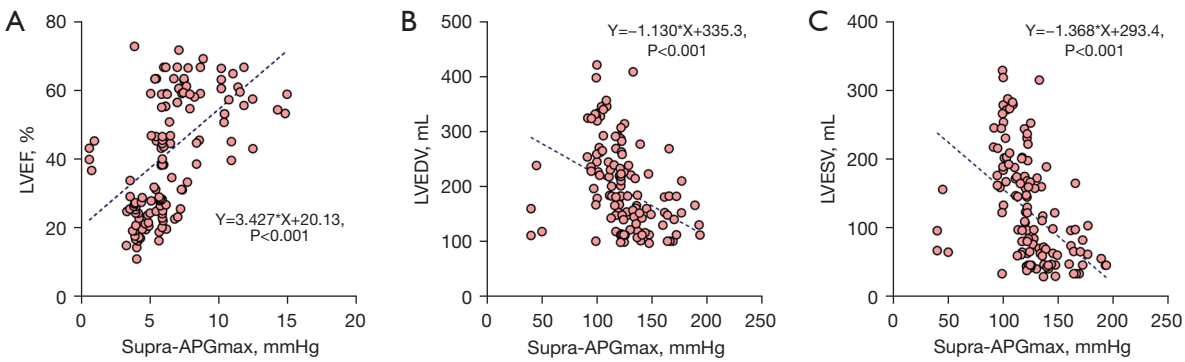

Figure 5 Rank correlation analysis between the pressure gradient across the aortic valve and cardiac function parameters. (A) Supra-APGmax was positively and linearly correlated with LVEF. (B) Supra-APGmax showed a negative linear correlation with LVEDV. (C) Supra-APGmax showed a negative linear correlation with LVESV. Supra-APGmax, pressure gradient across the aortic valve; LVEF, left ventricular ejection fraction; LVEDV, left ventricular end-diastolic volume; LVESV, left ventricular end-systolic volume.

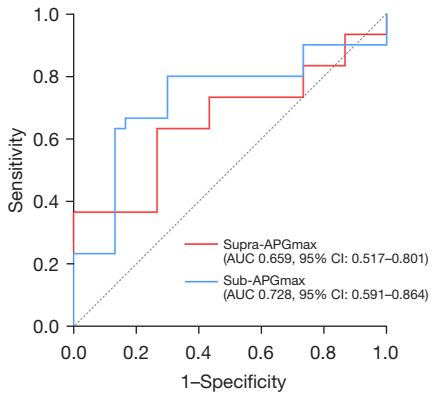

Figure 6 ROC curve for distinguishing HFpEF group from the control group using aortic valve pressure gradient. Supra-APGmax, aortic valve peak pressure gradient; Sub-APGmax, aortic valve subvalvular pressure gradient; AUC, area under the curve; CI, confidence interval; ROC, receiver operating characteristic; HFpEF, heart failure with preserved ejection fraction.

capable of accurately differentiating or providing clues for suspected cases would effectively reduce the risks of clinical misdiagnosis and oversight, offering significant benefits to patients. The differentiation of various HF types based on the pressure gradient of the LVOT in this study can help avoid subjecting patients to invasive examinations.

HF is characterized as a pathophysiological state where abnormal heart function leads to the heart's inability to pump blood at a rate sufficient to meet the body's metabolic demands under normal intracardiac pressures (18). Therefore, hemodynamic assessment of cardiac function abnormalities and ventricular remodeling is crucial in HF patients. Currently, the commonly used method for hemodynamic measurement is cardiac catheterization. However, guidelines from the Heart Failure Society of America (HFSA) advise against invasive hemodynamic quantification for patients with HFrEF (20). The use of echocardiography and 2D-phase-contrast (PC) CMR velocity measurements is limited by their single direction and plane, which may result in incomplete descriptions of intracardiac hemodynamics (21). Given that blood flow is a continuous 3D phenomenon, velocities, directions, and accelerations vary throughout the cardiac cycle. 4D flow CMR, which utilizes high temporal resolution 3D blood flow data, provides a comprehensive depiction of blood flow dynamics throughout the cardiac cycle. This includes peak velocities, transvalvular pressure gradients, wall shear stress, and vortices (22). In this study, quantitative analysis of left ventricular blood flow in HF patients using LVOT 4D flow CMR revealed that pressure gradients across the aortic valve, both supra- and subvalvular, demonstrate significant diagnostic capability for HF patients. These parameters are crucial for assessing the severity, progression, and treatment of HF.

The pathophysiology of HFrEF is complex, often originating from direct myocardial injury or underlying conditions such as coronary artery disease, myocardial infarction, and dilated cardiomyopathy, which result in impaired ventricular contraction (18). In this study, 4D flow CMR technology was employed to analyze intraventricular blood flow velocities across different types of HF patients. The findings revealed significantly lower peak velocities below the aortic valve in HF patients compared to healthy volunteers. Specifically, both HFrEF and HFmrEF patients exhibited reduced peak velocities below the aortic valve compared to the control group. Diminished intracavitary blood flow velocities in patients with reduced ejection fraction directly reflect myocardial injury and weakened ventricular contraction (23). Furthermore, the maintenance of blood flow dynamics in these patients is influenced by the pressure gradient generated by the heart (10). During contraction, increased ventricular and atrial pressures augment the pressure that propels blood forward (18). Reduced contractile function in HF patients indirectly contributes to lower pressure gradients. This study's analysis of pressure gradients in the LVOT demonstrated significantly diminished pressure gradients below the aortic valve in HF patients compared to healthy volunteers. This non-invasive finding provides insights into this mechanism. The pressure differential below the aortic valve drives ventricular ejection, and early detection of abnormalities in these parameters could facilitate better management and treatment strategies.

HFpEF is a clinical syndrome characterized by normal contraction of the LV but impaired relaxation during its diastolic phase (24). These relaxation abnormalities signify mechanical dysfunction in the heart muscle, involving slow or delayed relaxation, abnormal left ventricular expansion, and/or impaired filling of the LV (25). In this study, the quantitative analysis parameter used was the pressure gradient of the outflow tract, which decreases due to compromised ventricular expansion and filling. Patients with HFpEF may also experience vascular changes and cardiac remodeling, which can disrupt the normal relationship between afterload and diastolic duration, leading to an imbalance between myocardial oxygen supply and demand,

potentially resulting in ischemia (26). This ischemia reduces blood flow within the heart chambers, including the vicinity of the aortic valve, aligning with the findings of this study. The diagnosis of HFpEF, characterized by diastolic dysfunction, has long posed challenges for clinicians. Through the analysis of outflow tract blood flow parameters, this study demonstrates that pressure gradients above and below the aortic valve can effectively differentiate between HFpEF patients and healthy volunteers, as indicated by their performance in ROC curves. However, further validation is necessary to ensure the accuracy and clinical applicability of these findings.

Limitations

This study has the following limitations and potential future directions:

The study did not include invasive pressure measurements, thus heart load conditions remained unknown. Patients in the study group were older compared to those in the control group, and previous studies have shown that EDV, ESV, and SV tend to decrease with increasing age. The sample size for modeling in this study was relatively small and will be expanded in future research. Lastly, further investigation is needed to assess the effectiveness of 4D flow CMR technology in evaluating HF due to various etiologies or influencing factors. Additional limitations include the restricted spatial and temporal resolution of 4D flow MRI. Moreover, 4D flow MRI data are acquired over multiple cardiac cycles and then averaged, which may affect the estimation of maximum velocity.

Conclusions

Based on the acquired 4D flow data from inflow and outflow tracts, this study enables visual analysis of intraventricular blood flow and provides clear observation of the blood flow's trajectory during the cardiac systolic phase. The pressure gradient above the aortic valve during systole is valuable in distinguishing between different types of HF, offering insights for early diagnosis and prognostic evaluation.

Acknowledgments

We would like to thank all the participants and staff involved in the CMR scanning, image collection, and data post-processing performed by this investigator.

Funding: This study received funding by the National Key R&D Program of China (No. 2022YFC2010003) and the National Natural Science Foundation of China (2021 NSFC: 82160333).

Footnote

Reporting Checklist: The authors have completed the STROBE reporting checklist. Available at https://qims.amegroups.com/article/view/10.21037/qims-24-311/rc

Conflicts of Interest: All authors have completed the ICMJE uniform disclosure form (available at https://qims.amegroups.com/article/view/10.21037/qims-24-311/coif). X.Y. is an employee of Philips Healthcare. The other authors have no conflicts of interest to declare.

Ethical Statement: The authors are accountable for all aspects of the work in ensuring that questions related to the accuracy or integrity of any part of the work are appropriately investigated and resolved. The study was conducted in accordance with the Declaration of Helsinki (as revised in 2013). The study was approved by the Research Ethics Committee of Ningxia Medical University General Hospital (approval No. KYLL-2021-255) and the requirement for individual consent for this analysis was waived due to retrospective nature of this study.

References

1. Heidenreich PA, Bozkurt B, Aguilar D, Allen LA, Byun JJ, Colvin MM, et al. 2022 AHA/ACC/HFSA Guideline for the Management of Heart Failure: A Report of the American College of Cardiology/American Heart Association Joint Committee on Clinical Practice Guidelines. J Am Coll Cardiol 2022;79:e263-421.
2. Nagueh SF, Smiseth OA, Appleton CP, Byrd BF 3rd, Dokainish H, Edvardsen T, Flachskampf FA, Gillebert

TC, Klein AL, Lancellotti P, Marino P, Oh JK, Alexandru Popescu B, Waggoner AD; Houston, Texas; Oslo, Norway; Phoenix, Arizona; Nashville, Tennessee; Hamilton, Ontario, Canada; Uppsala, Sweden; Ghent and Liège, Belgium; Cleveland, Ohio; Novara, Italy; Rochester, Minnesota; Bucharest, Romania; and St. Recommendations for the Evaluation of Left Ventricular Diastolic Function by Echocardiography: An Update from the American Society of Echocardiography and the European Association of Cardiovascular Imaging. Eur Heart J Cardiovasc Imaging 2016;17:1321-60.
3. McDonagh TA, Metra M, Adamo M, Gardner RS, Baumbach A, Bohm M, et al. 2021 ESC Guidelines for the diagnosis and treatment of acute and chronic heart failure. Eur Heart J 2021;42:3599-726.
4. Chacon-Portillo MA, Acharya T, Janardhanan R. Imaging in heart failure with preserved ejection fraction: insights into echocardiography and cardiac magnetic resonance imaging. Rev Cardiovasc Med 2021;22:11-24.
5. Bissell MM, Raimondi F, Ait Ali L, Allen BD, Barker AJ, Bolger A, et al. 4D Flow cardiovascular magnetic resonance consensus statement: 2023 update. J Cardiovasc Magn Reson 2023;25:40.
6. Ebel S, Köhler B, Aggarwal A, Preim B, Behrendt B, Jung B, Gohmann RF, Riekena B, Borger M, Lurz P, Denecke T, Grothoff M, Gutberlet M. Comparison of aortic blood flow rotational direction in healthy volunteers and patients with bicuspid aortic valves using volumetric velocity-sensitive cardiovascular magnetic resonance imaging. Quant Imaging Med Surg 2023;13:7973-86.
7. Kollmeier JM, Kalentev O, van Zalk M, Voit D, Frahm J. Maximum velocity projections within 30 seconds: a combination of real-time three-directional flow MRI and cross-sectional volume coverage. Quant Imaging Med Surg 2023;13:3307-15.
8. Carlsson M, Heiberg E, Toger J, Arheden H. Quantification of left and right ventricular kinetic energy using four-dimensional intracardiac magnetic resonance imaging flow measurements. Am J Physiol Heart Circ Physiol 2012;302:H893-900.
9. Nakaji K, Itatani K, Tamaki N, Morichi H, Nakanishi N, Takigami M, Yamagishi M, Yaku H, Yamada K. Assessment of biventricular hemodynamics and energy dynamics using lumen-tracking 4D flow MRI without contrast medium. J Cardiol 2021;78:79-87.
10. Hsu S, Fang JC, Borlaug BA. Hemodynamics for the Heart Failure Clinician: A State-of-the-Art Review. J Card Fail 2022;28:133-48.
11. Kanski M, Arvidsson PM, Töger J, Borgquist R, Heiberg E, Carlsson M, Arheden H. Left ventricular fluid kinetic energy time curves in heart failure from cardiovascular magnetic resonance 4D flow data. J Cardiovasc Magn Reson 2015;17:111.
12. van Ooij P, Allen BD, Contaldi C, Garcia J, Collins J, Carr J, Choudhury L, Bonow RO, Barker AJ, Markl M. 4D flow MRI and T1 -Mapping: Assessment of altered cardiac hemodynamics and extracellular volume fraction in hypertrophic cardiomyopathy. J Magn Reson Imaging 2016;43:107-14.
13. Metra M, Teerlink JR. Heart failure. Lancet 2017;390:1981-95.
14. Suzuki M, Kotooka N, Sakuma M, Nakazono T, Node K, Irie H. Validity and Reliability of Three-chamber-View Three-directional Encoded Phase-contrast Magnetic Resonance Velocity-Vector Mapping for Transmitral Velocity Measurements: Comparison with Doppler Echocardiography and Intra- and Inter-observer Variability. Magn Reson Med Sci 2017;16:152-8.
15. Cawley PJ, Maki JH, Otto CM. Cardiovascular magnetic resonance imaging for valvular heart disease: technique and validation. Circulation 2009;119:468-78.
16. Sheth PJ, Danton GH, Siegel Y, Kardon RE, Infante JC Jr, Ghersin E, Fishman JE. Cardiac Physiology for Radiologists: Review of Relevant Physiology for Interpretation of Cardiac MR Imaging and CT. Radiographics 2015;35:1335-51.
17. Pandey A, Parashar A, Kumbhani D, Agarwal S, Garg J, Kitzman D, Levine B, Drazner M, Berry J. Exercise training in patients with heart failure and preserved ejection fraction: meta-analysis of randomized control trials. Circ Heart Fail 2015;8:33-40.
18. Bloom MW, Greenberg B, Jaarsma T, Januzzi JL, Lam CSP, Maggioni AP, Trochu JN, Butler J. Heart failure with reduced ejection fraction. Nat Rev Dis Primers 2017;3:17058.
19. Savarese G, Stolfo D, Sinagra G, Lund LH. Heart failure with mid-range or mildly reduced ejection fraction. Nat Rev Cardiol 2022;19:100-16.
20. Heart Failure Society of America; Lindenfeld J, Albert NM, Boehmer JP, Collins SP, Ezekowitz JA, Givertz MM, Katz SD, Klapholz M, Moser DK, Rogers JG, Starling RC, Stevenson WG, Tang WH, Teerlink JR, Walsh MN. HFSA 2010 Comprehensive Heart Failure Practice Guideline. J Card Fail 2010;16:e1-194.
21. Ashkir Z, Myerson S, Neubauer S, Carlhäll CJ, Ebbers T, Raman B. Four-dimensional flow cardiac magnetic

resonance assessment of left ventricular diastolic function. Front Cardiovasc Med 2022;9:866131.
22. Corrias G, Cocco D, Suri JS, Meloni L, Cademartiri F, Saba L. Heart applications of 4D flow. Cardiovasc Diagn Ther 2020;10:1140-9.
23. Alattar Y, Soulat G, Gencer U, Messas E, Bollache E, Kachenoura N, Mousseaux E. Left ventricular diastolic early and late filling quantified from 4D flow magnetic resonance imaging. Diagn Interv Imaging 2022;103:345-52.
24. Dusch MN, Thadani SR, Dhillon GS, Hope MD. Diastolic function assessed by cardiac MRI using longitudinal left ventricular fractional shortening. Clin Imaging 2014;38:666-8.
25. Gaasch WH, Zile MR. Left ventricular diastolic dysfunction and diastolic heart failure. Annu Rev Med 2004;55:373-94.
26. Kawaguchi M, Hay I, Fetics B, Kass DA. Combined ventricular systolic and arterial stiffening in patients with heart failure and preserved ejection fraction: implications for systolic and diastolic reserve limitations. Circulation 2003;107:714-20.

Cite this article as: Guo J, Yue X, Liang W, Ma L, Sun X, Zhang H, Zhu L. The value of blood flow velocity and pressure gradient in differentiating patients with different types of heart failure. Quant Imaging Med Surg 2024;14(10):7612-7624. doi: 10.21037/qims-24-311